The Fabrication and Electrocaloric Effect of Bimodal-Grain Structure $(Ba_{0.60}Sr_{0.40})TiO_3$ Using the Induced Abnormal Grain Growth Method

IOP Conf. Series: Materials Science and Engineering **678** (2019) 012138 doi:10.1088/1757-899X/678/1/012138

The Fabrication and Electrocaloric Effect of Bimodal-Grain Structure $(Ba_{0.60}Sr_{0.40})TiO_3$ Using the Induced Abnormal Grain Growth Method

H F Zhang[1], X Chen[2], J Gao[3], K H Lam[4], S D Liang[4], L F Fei[5], C L Mak[5] and J F Chen[6]

[1]Department of Physics, Suzhou University of Science and Technology, Suzhou 215009, China

[2]Department of materials science and engineering, The Pennsylvania State University Park, PA 16802, USA

[3]School of Optoelectronic Engineering, Zaozhuang University, Zaozhaung, Shandong, 277160, China

[4]Department of Electrical Engineering, The Hong Kong Polytechnic University, Hung Hom, Kowloon, Hong Kong

[5]Department of Applied Physics, The Hong Kong Polytechnic University, Hung Hom, Kowloon, Hong Kong

[6]Suzhou institute of Nano-tech and Nano-bionics, Chinese Academy of Science, Suzhou, 215123, China

E-mail: constance_zhanghf@126.com

Abstract. Bimodal-grain structure $(Ba_{0.6}Sr_{0.4})TiO_3$ ceramics had been prepared using induced abnormal grain growth method (IAGG). Two grain size distributions, between 10 ~ 20 μm and 100 ~ 300 μm, were found during the sintering temperature of 1250 ~ 1350°C. Our results suggested that the ultra-large grain exhibited the high dielectric and ferroelectric properties comparable to the single crystal. At the same time, the fine-grain caused a phase diffusion transition at the Curie temperature about 20°C. The direct measured electrocaloric effect showed that the best performance is achieved with ΔT of 0.6 K, and ΔS of 1.02 J $kg^{-1}K^{-1}$ near room temperature and electric field strength of 2 MV/m.

1. Introduction

The electrocaloric effect (ECE) refers to the temperature as well as entropy change of an insulating material when there is an electric field induced polarization change [1-3]. The ECE of ferroelectrics has attracted a lot of interest due to its potential applications in solid-state refrigeration, which is regarded as the best solution for cooling microelectronic devices due to the easy of miniaturization, high efficiency and low cost [4]. From the considerations on the performance of the device, a "good" ECE material should possess (1) large ECE induced entropy change (ΔS) and adiabatic temperature change (ΔT) under a reasonable electric field strength; and (2) large working temperature range of the ECE material [5-8]. Therefore, one critical question is how to design and develop dielectric materials which are capable of generating giant ECE over a broad operation temperature with relatively low

applied electric field. A thorough review of the state-of-the-art electrocaloric research reveals relaxor ferroelectrics could be a suitable material system as a solid-state working body because they present large ECEs with much mild temperature dependencies [9; 10].

Theoretically works on the ECE indicate that larger grain sized should promote the ECE, because the grain boundaries have weaker ferroelectricity than that of the grains, besides the intrinsic nature of the material [11-14]. Among various ferroelectrics, $Ba_{1-x}Sr_xTiO_3$ ferroelectric, as an environmental friendly materials, have been given much attention due to their excellent electrical properties. It is one of the promising candidates for electrocaloric refrigeration because its Curie temperature can be easily controlled by means of Sr content, implying that it can realize a large ECE near room temperature. Therefore, control of the grain size may be used to achieve substantial enhancement of the ECE with a properly engineered microstructure of $Ba_{1-x}Sr_xTiO_3$ ceramic [11; 13].

In this study, inspired by the new Twin peaks building (Sydney, Australia), which preserves the parent characteristics, while at the same time creates a unique style. We introduced an induced abnormal grain growth method (IAGG) to develop the bimodal-grain structure $Ba_{0.60}Sr_{0.40}TiO_3$ (BST) ceramic. The high dielectric properties can be achieved by ultra-large size grains to enhance the ECE performance. At the same time, the fine-sized grains can cause the phase transition diffusion at the transition temperature T_C similar to the relaxor behavior, ensuring the large ECE performance over a broad temperature. Preparation and microstructure characterization, together with the dielectric properties and ECE performance of bimodal-grain structure BST will be investigated in a detail way.

2. Experimental procedure

2.1. Preparation Proceeding of IAGG method

BST powder with a Ba/Sr ratio of 60/40 was synthesized by using the conventional solid-state reaction from barium titanate ($BaTiO_3$) and strontium titanate ($SrTiO_3$) at 1175^{o}C for 7 h. The BST 60/40 powder was then milled for 24 h with a normal planetary ball milling, followed by drying at 120^{o}C for 12 h. The resulted powder was denoted as 1175-BST. Meanwhile, BST 60/40 gel powder was prepared by using the method that has been reported previously by the authors [15]. The BST60/40 gel powder was dried at 120^{o}C for 12 h and denoted as Gel-BST. Afterwards, powders of 1175-BST and Gel-BST were mixed by IAGG method through a hybrid processing [16-18]. In this study, the ratio of 1175-BST (the filler) and Gel-BST (the matrix) was kept at 10 wt%：90 wt%. The mixture was mixed thoroughly for 12 h in isopropyl alcohol solvent as milling agent to form a uniform slurry, which was then dried at 120^{o}C for 24 h. Finally, the dried powder was used to prepare green pellets without granulation. All the green pellets with a diameter of 10 mm and thickness of 1 mm, were sintered between 1100 ~ 1400^{o}C for 2 h at a heating rate of 2^{o}C/min.

2.2. Characterization

Phase composition of the powders and the sintered ceramics were examined by using X-ray diffraction (XRD, Bruker D8 ADVANCE) with CuKα1 radiation (1.5418 Å, 40 kV, 40 mA) at a scan step of 0.02º at room temperature. Morphology of the ceramics was observed by using scanning electron microscopy (SEM, JEOL JSM-6490). To measure the dielectric and ferroelectric properties, Ag was coated as electrodes. The temperature dependent dielectric spectrum was measured at 1-100 kHz using a dielectric temperature analyzer (RT-800, TZDM) from -10°C to 150°C at a rate of 1°C/ min rate. The polarization-electric field hysteresis loops were evaluated using a modified Sawyer Tower circuit operated at a frequency of 100 Hz at 10^{o}C.

3. Results and discussion

3.1. Sinterability and Microstructure

Figure 1 shows the morphology development of the BST ceramics grown by IAGG method as a function of sintering temperature, including the size distribution sintered at 1350^{o}C and 1400^{o}C, respectively.

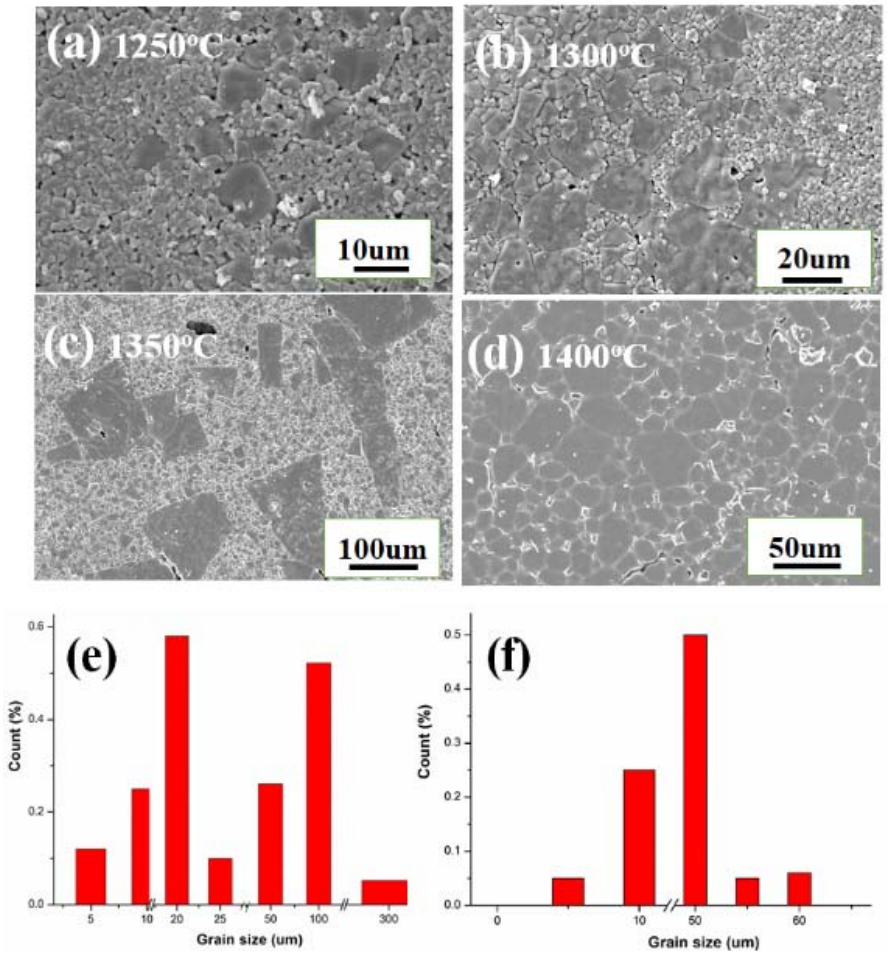

Figure 1. The surface morphology evolution of the BST ceramics at the sintering temperatures of 1230–1400°C for 2 h (a-d); together with the typical size distributions in 1350°C(c) and 1400°C(d), respectively.

As observed in Figures 1 (a) and (b), with the sintering temperature increased from 1250 to 1300°C, it is interesting to find a small amount of grains growing up with sizes of about 10 ~ 20 μm, which are surrounded by those of submicron-size grains of about 1-2 μm in the matrix. We believe that the small number of coarse grains were derived from the filler (i.e., the micron-size 1175-BST powder). When the sintering was increased to 1350°C, these relatively large grains begin to be exaggerated and elongated. Eventually, ultra-large grains with sizes of about 100-300 μm were formed. However, when the sintering temperature was increased to 1400°C, the ceramics exhibited nearly homogeneous microstructure, with grain sizes in the range of 20–50 μm. As shown in Figures 1(a)-(c), BST ceramics demonstrated a non-uniform growth exhibiting an obvious bimodal-grain structure.

The grain growth phenomena can be explained as following: it is known that the grain growth rate (the movement of grain boundary) is approximately proportional to a free-energy difference (ΔG) across a curved grain boundary as shown in equation (1) [19]:

$$\Delta G = \gamma \bar{V}(\frac{1}{r_1} + \frac{1}{r_2}) \quad (1)$$

where ΔG is the change in free energy on going across the curved interface, γ is the boundary energy, $\bar{V}$is the molar volume, and r_1 and $r_2$are the principal radii of curvature. The rate of growth of large grains is dependent on the number of grain sides [20], the ball-milled irregular 1175-BST filler [15]

regarded as a nucleus with many more sides is present at the beginning of recrystallization in the Gel-BST matrix, the filler powder grows more rapidly than the neighboring small gains with fewer sides originated from Gel matrix due to the much large curvature, which ΔG is the driving force that makes the boundary move toward its center of curvature. At the same time, the jumping probability of atoms from the smaller grains with convex side surface to giant grains with concave side surface is larger than that from the concave side surface to the convex side surface [20]. As a result, the giant grain can easily grow by absorbing the surrounding small grains owing to induced abnormal grain growth (IAGG). When the elevated sintering temperature reached to 1350°C, the giant grain growth reached its critical size with the apparently perfectly straight boundaries with low surface energy (curvature is near to zero) as shown in Figure 1(c). Therefore, the grain growth stops when the boundaries of giant grains meet, the uniform grain size i.e. normal grain growth (NGG) was observed when the sintering temperature was increased to 1400°C. This morphology evolution illustrates that grain growth of the large-sized grains proceeded to a rate nearly proportional to $1/d_m$ (d_m is the average grain size of matrix) during the sintering temperatures of 1350 ～1400°C. Therefore, the rate of filler grain growth decreasedand would keep constant as long as the d_m remained unchanged [20], resulting in a uniform microstructure with relatively smaller grains appeared again.

Furthermore, the existence of straight-line grain boundaries observed in Figure 1(c) suggests that there is a crystal axis which the grain growth easily occurs along. The formation process of the ultra-large single grains by using our IAGG method is similar to "cloning" the fillers, while the gel matrix is just like the "nutrient source or reservoir" to breed the fillers to grow up. Thus, by adding fillers with longitudinal direction coincide with the crystal axis in the Gel-matrix, the fillers may grow along the axis so that an oriented fillers single crystal will be obtained by the IAGG method. Therefore, our finding suggests that well-controlled microstructure with bimodal-grain structure $Ba_{1-x}Sr_xTiO_3$ with over the whole composition range can be produced in an easy and simple way using the IAGG method. Besides $Ba_{1-x}Sr_xTiO_3$, this novel method ought to be useful also in controlling the well-defined microstructures of many other ferroelectric perovskite-type crystals.

Figure 2 shows XRD patterns of the 1175-BST powder and the two groups of ceramics sintered at 1350°C. As shown in Figure 2, all the samples had a typical single perovskite phase without the presence of secondary phases, all the peaks can be coincide with the diffraction indexes of BST.

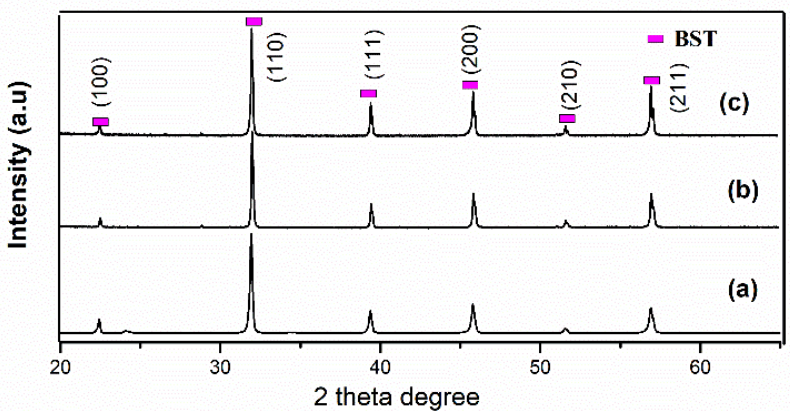

Figure 2. XRD patterns of 1175-BST powder(a); the two groups of ceramics sintered at 1350°C for 2 h prepared by Gel-BST matrix by sol-gel technique (b) and mixed powder by IAGG method (c).

3.2. Curie Temperature and ferroelectricity

Figure 3 shows the temperature dependent dielectric constant of a typical IAGG sample sintered at 1350°C in the temperature range of 0 to120°C at three selected frequencies (1 kHz,10 kHz, 100 kHz and 1MHz), including (b) the polarization-field hysteresis loop (P-E) at 100 Hz and 10°C. As shown in

Figure 3(a), the Curie temperatures are about 20°C, with a dielectric constant of 9754 at 10 kHz. Usually, the Curie temperature of BST ceramics produced by conventional ceramic processing or sol-gel technique at 1350°C is below 10°C [21]. The increased Curie temperature and high dielectric constant by IAGG present in here are ascribed to the bimodal-grain structure, that is, ultra-large grains (i.e. single crystal) dominate dielectric properties of the ceramics.

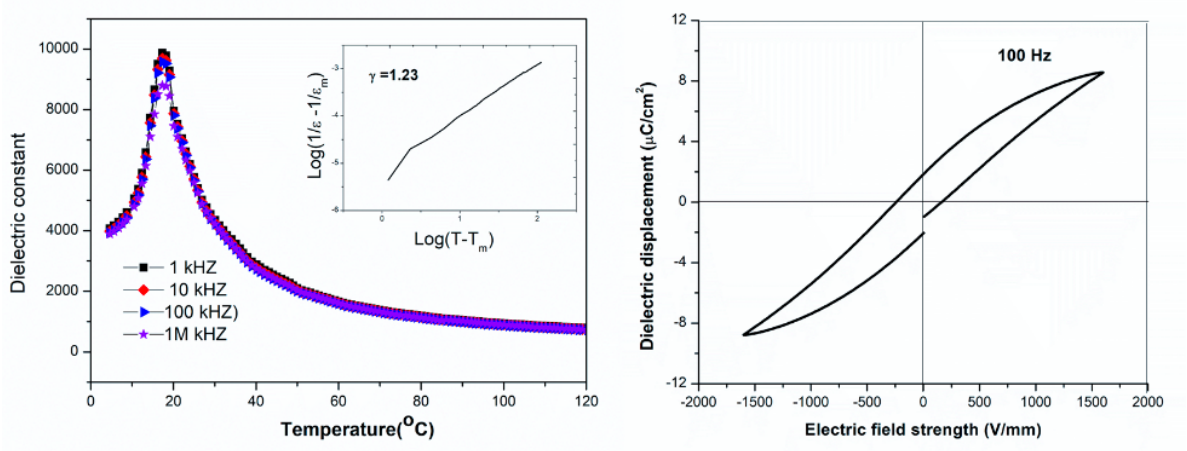

Figure 3. Dielectric constant and loss tangent as a function of frequency(a) and ferroelectric hysteresis loops at 100 Hz and 10°C (b). Dashed lines are drawn to guide the eye, including the inset in Figure 3(a) showing the plot of log(1/ε−1/ε_m) as the function of log(T−Tm) at 100 kHz.

Additionally, it is noticed that the Curie temperature observed in Figure 3(a) is a little widened and acts a diffused phase transition. For the relaxor ferroelectrics, the reciprocity of the dielectric constant and temperature follows the Uchino and Nomura function, a modified Curie–Weiss law as shown in equation (2) [22],

$$\frac{1}{\varepsilon} - \frac{1}{\varepsilon_m} = \frac{(T - Tm)^{\gamma}}{C} \tag{2}$$

where C is the Curie constant and γ is a diffusion coefficient ranging from one (a normal ferroelectric) to two (an ideal relaxor ferroelectric). The plot of log(1/ε−1/ε_m) as the function of log(T−Tm) at 100 kHz was given in the inset of Figure 3(a). The slope of fitting curves is used to determine the γvalue. It can be calculated that γ = 1.23, compared to the sharp peak occurred in Curie temperature previously reported $Ba_{0.65}Sr_{0.35}TiO_3$ single crystal [23], we believe that the fine-grain size distribution in bimodal-grain structure contributed to the diffuse phase transition behavior.

In Figure 3(b), the hysteresis loop shows the reasonable ferroelectric properties of the BST60/40 ceramic fabricated by the IAGG method. The values of P_s, P_r and $E_c$are found to be at about 8.65 μC/cm^2, 1.79 μC/cm^2 and 0.17 kV/mm at 100 Hz and 10°C, respectively. These properties are close to those in $Ba_{0.65}Sr_{0.35}TiO_3$ single crystal [23]. These results confirm that bimodal-grain structure presented in here can preserve the parent characteristics, on the other hand, the amounts of bimodal grains can exhibit its unique properties.

3.3. ECE performance

The typical thickness of bulk sample used in the ECE measurement was 200 μm. The direct ECE measurement was carried out via the thermistor and a high resolution calorimeter recording heat flux induced by the temperature change of EC materials under electrical field [24]. The heat generated by the ECE sample is compared with the heat generated by a standard reference resistor R, from which ΔS determined. When a constant voltage, V, with a pulse time duration, t (<0.5 seconds), is applied to

a reference resistor (Top electrode) heater R, a joule heat $Q_h=(V^2/R)t$ is produced. The heat generated is detected by a heat flux sensor directly attached to the sample surface. Now, if the ECE sample under an applied electric field also generates the same amount of heat as detected by the same flux sensor, then the heat Q_{ECE} from the ECE material is equal to Q_h. From $Q_h= Q_{ECE}=T\Delta S$, ΔS, the isothermal entropy change can be obtained. If the ECE material has a specific heat capacity of c_E, a densityρ, and a volume of V, then the adiabatic temperature change (ΔT) can be obtained, $\Delta T= Q_{ECE}/c_E\rho V$. On the basis of these measurements, ECE as function of both temperature and applied electric field E were characterized.

Figure 4 shows (a) the V-t curve and (b) the heat detected by heat flux sensor of the reference resistor, and (c) the direct recorded ECE signal for BST as the electric field was turning on and off. Based on the Figure 4, the adiabatic temperature change (ΔT) and isothermal specific entropy change (ΔS) were induced under different electric field strength at room temperature shown in Figure 5.

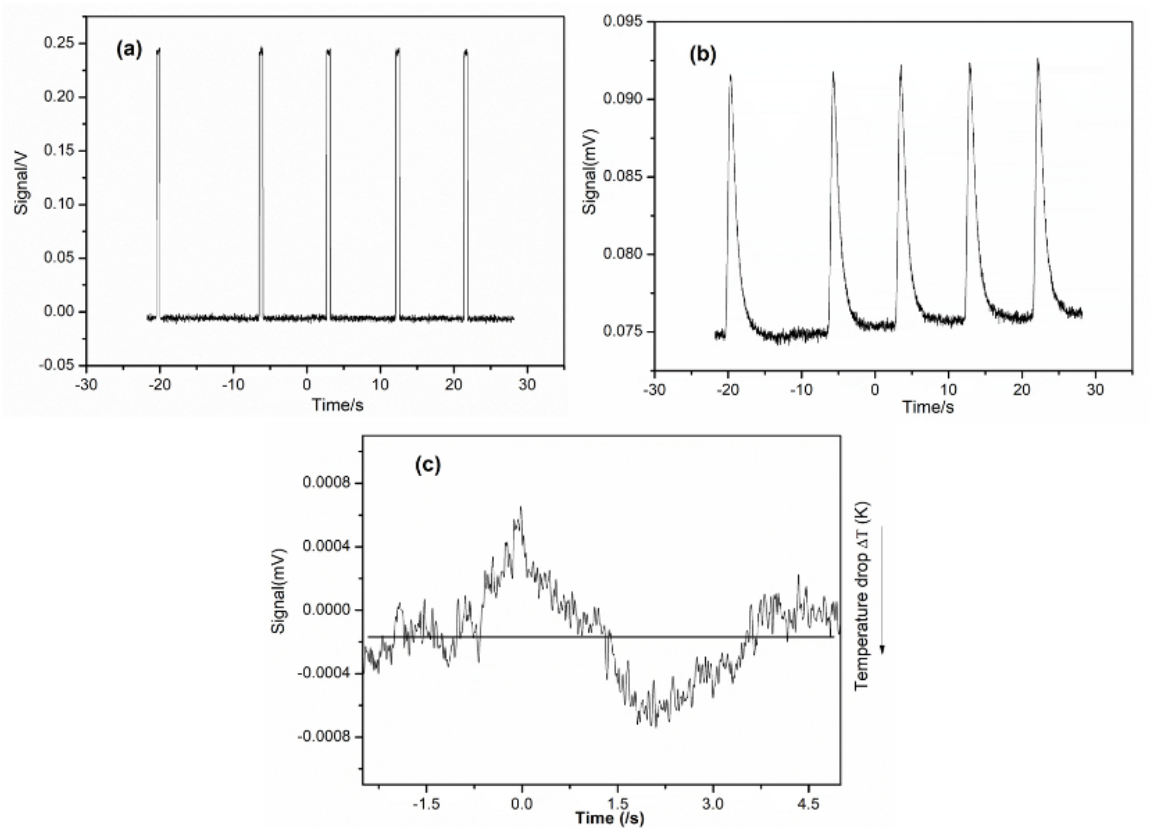

Figure 4. The Voltage(V)- time (s) curve of the reference resistor(a); the heat recorded by heat flux sensor of reference resistor versus time(b) and the direct recorded ECE signal for BST as the electric field was turning on and off (c).

In Figure 5, the maximum ΔT was reached to 0.6 K, and ΔS is 1.02 J/kg·K under E = 2 MV/m and room temperature, showing the best performance. By comparison, the present ECE performance is the 3 times higher that the value reported previously (ΔT_{max} is about 0.23K at E=2MV/m near room temperature) [11]. We believe that the better performance can be contributed to the combination of ultra-large grains and fine-grain leading to the larger ECE, in which the characteristics of large grains is similar to the single crystal with the same composition, while fine-grains can mitigate the peak of Curie temperature inducing the phase diffusion.

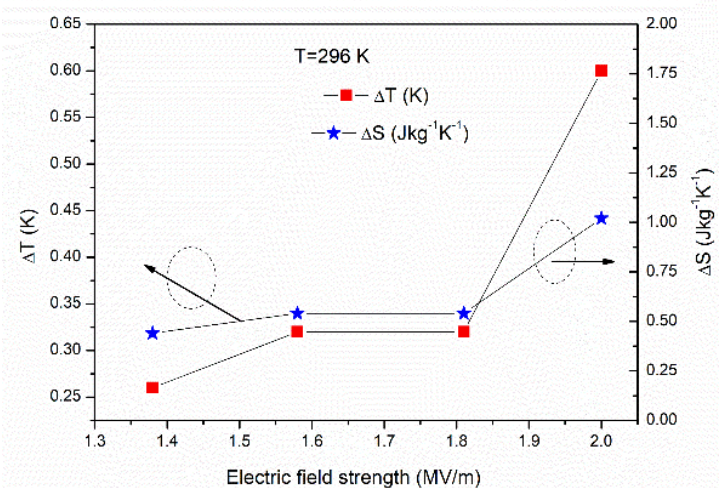

Figure 5. ΔT and ΔS was measured under different electric field strength at room temperature.

4. Conclusions

A new bimodal-grain structure of BST has been fabricated successfully by the IAGG method, and our finding suggests that large-sized grain exhibited the single crystal characteristics with high dielectric and ferroelectric properties; while, the fine-grains cause the diffusion phenomena occurred at Curie temperature, similar to relaxor behavior in bimodal-grain structure. The ECE performance shows the ΔT reached to 0.6 K, and ΔS was 1.02 J/kg·K under E = 2 MV/m and room temperature. Also, the novel IAGG method could be used as a reference to fabricate high quality bimodal-grain structure of other ferroelectric materials simply、reproducibly and inexpensively at relatively low temperature.

Acknowledgements

This work was supported by research funding from Suzhou University of science and technology, and The Hong Kong Polytechnic University (1-ZVGH), and the National Natural Science Foundation of China (Grants no. 11574227).

References

[1] Birks E, Dunce M and Sternberg A 2010 *Ferroelectrics* **400** 336
[2] Neese B C, Chu B J, Lu S G, Y Wang, Furman E and Zhang Q M 2008 *Science* **321** 821
[3] Mischenko A S, Zhang Q, Scott J F, Whatmore R W and Mathur N D 2006 *Science* **311** 1270
[4] Gu H 2014 *Chip-scale cooling devices based on electrocaloric effect* (Dissertation, The Pennsylvania State University)
[5] Gu H, Craven B, Qian X S, Li X, Cheng A, and Zhang Q M 2013 *Appl.Phys. Lett.* **102** 112901
[6] Gu H, Qian X S, Li X, Craven B, Zhu W, Cheng A, Yao S C and ZhangQ M 2013 *Appl. Phys. Lett.* **102** 122904
[7] Ju Y S J 2010 *Electron. Packag.* **132** 041004
[8] Jia Y and Ju Y S 2012 *Appl. Phys. Lett.* **100** 242901
[9] Lu S G and Zhang Q M 2009 *Adv. Mater.***21** 1983
[10] Shi J, Han D, Li Z, Yan L, Lu S G, Zhong Z, Chen J, Zhang Q M and Qian X 2019 *Joule* **3** 1
[11] Bai Y, Han X, Ding K and Qiao L J 2013 *Appl. Phys. Lett.* **103** 162902
[12] Qiu J H and Jiang Q 2009 *J. Appl. Phys.* **105** 034110
[13] Vrabelj M, Ursic H, Kutnjak Z, Rozica B, Drnovsek S, Bencan A, Bobnar V, Lovro Fulanovic L and Malic B 2016 *J. Eur. Ceram. Soc.* **36** 75
[14] Xu Z and Qiang H 2017 *Mater. Lett.* **191** 57
[15] Zhang H, Yao X and Zhang L 2007 *J. Am. Ceram. Soc.* **90** 2333

[16] Zhang H, Or S W, Chan H L W and Yang F 2011 *J. Eur. Ceram. Soc.* **31** 1753
[17] Zhang H, Or S W and Chan H L W2008 *J. Appl. Phys.* **104** 104109
[18] Zhang H, Mak C L, Chan H L W and Yao X 2013 Sintering Applications *Low temperature hybrid processing technology of fine electronicceramics* (InTech Open Access Publisher, Croatia) Chapter 6 pp119-142
[19] Eda K, Inada M and Matsuoka M 1983 *J. Appl. Phys.* **54** 1095
[20] Kingery W D, Bowen H K and Uhlmann D R 1976 *Introduction to Ceramics*. *2nd ed*. (Wiley, New York) pp464
[21] Zhang H 2005 *Study on the preparation and dielectric properties of* Barium Strontium Titanate ceramics and thick films (Dissertation, Tongji University)
[22] Uchino K and Nomura S 1982 *Ferroelectr. Lett. Sect.* **44** 55
[23] Henson R M and Pointon A J 1974 *J. Cryst. Growth* **26** 174
[24] Li X, Qian X S, Lu S G, Cheng J, Fang Z and Zhang Q M 2011 *Appl. Phys. Lett.* **99** 052907